Sidewall Boundary-Layer Corrections in Subsonic, Two-Dimensional Airfoil/Hydrofoil Testing

A. L. Treaster* and G. B. Gurney†
The Pennsylvania State University, State College, Pennsylvania
and
P. P. Jacobs Jr.‡
Edwards Air Force Base, California

Historically, in water or wind tunnels without sidewall boundary-layer control, balance-measured lift and pitching moment data have been acceptable, whereas drag data have varied by as much as an order of magnitude from previous reference data. An experimental wind tunnel program was conducted to investigate the parameters that influence these subsonic, two-dimensional, balance-measured airfoil/hydrofoil section characteristics. From the results of this program, the sidewall boundary layer was identified as the primary factor contributing to the erroneous drag measurements. A correction procedure based on the airfoil/hydrofoil geometry, the flow environment, and the measured data was developed. Corrected data from the subject test program and from similar programs in other experimental facilities for both symmetrical and cambered sections are in good agreement with the reference data.

Nomenclature

$\mathcal{R}$ = aspect ratio = s^2/sc
b = exponent in Eq. (11)
c = airfoil chord length
c_d = sectional drag coefficient, = $D/(q_\infty c)$
c_{d_0} = sectional drag coefficient at $c_\ell = 0.0$
c_ℓ = sectional lift coefficient, = $L/(q_\infty c)$
c_{ℓ_α} = local slope of the c_ℓ vs α curve
$c_{\ell_{\alpha-0}}$ = slope of the linear portion of the c_ℓ vs α curve (usually evaluated in the $c_\ell = 0.0$ region)
D = drag force
D_e^* = Hawthorne's approximation of the energy in a secondary flow [Eq. (1)]
$f(n)$ = defined by Eq. (2) and Fig. 10
g_i = functional operators used in developing Eq. (12)
K_i = proportionality constant used in developing Eq. (12)
L = lift force
n = defined by Eq. (3)
P_{atm} = atmospheric pressure
P_s = static pressure
P_{total} = total pressure
q = local dynamic pressure, = $\frac{1}{2}\rho u^2$
q_∞ = freestream dynamic pressure, = $\frac{1}{2}\rho V_\infty^2$
Re = Reynolds number, = $V_\infty c/\nu$
s = airfoil span
t = maximum airfoil thickness
u = local velocity
V_∞ = freestream velocity
x = distance parallel to test section centerline measured from the leading edge of the two-dimensional test chamber
α = airfoil angle of attack
Δc_d = required correction to c_d
δ = test section wall boundary-layer thickness at the centerline of the balance shaft
δ^* = test section wall boundary layer displacement thickness at the centerline of the shaft
ρ = mass density of the fluid
ν = kinematic viscosity of the fluid

Presented as Paper 84-1366 at the AIAA/SAE/ASME 20th Joint Propulsion Conference, Cincinnati Ohio, June 11-13, 1983; received July 9, 1984; revision received Oct. 19, 1984. The paper is declared a work of the U.S. Government and therefore is in the public domain.

*Research Associate, Applied Research Laboratory.
†Assistant Professor, Applied Research Laboratory.
‡Flight Test Engineer, United States Air Force. Member AIAA.

Introduction

THE use of a force balance to measure simultaneously the sectional characteristics of an airfoil or hydrofoil that spans a rectangular test section has met with only partial success. Although the lift and pitching moment data have usually been acceptable, the drag data (with the traditional corrections applied) have varied by as much as an order of magnitude from established reference data. Based on studies conducted in the subsonic wind tunnel of the Applied Research Laboratory at The Pennsylvania State University (ARL/PSU) the sidewall boundary layer was identified as the primary factor contributing to these erroneous drag measurements. Presented herein is an empirically derived method to correct for the presence of the sidewall boundary layer in subsonic two-dimensional airfoil/hydrofoil testing with a mechanical force balance.

A review of the literature indicated that most of the currently used NACA airfoil section data were measured in wind tunnels during the 1930's and 1940's. The majority of these data were acquired by measuring individually the lift, drag, and pitching moment by the most accurate means available. Generally, this required either the measurement of the pressure distributions on the ceiling and floor of the test section or the use of a force balance to obtain lift. Drag data were obtained from either wake surveys or via surface pressure distributions; a torsional balance was usually used to measure the pitching moment. Typical of these measurements programs were those conducted by Loftin and Smith[1] in 1949.

In wind tunnel testing, the sidewall boundary layer can sometimes be managed by blowing or suction techniques. More recently computational procedures, such as those by Barnwell,[2] Sewall,[3] and Kemp and Adcock,[4] have been applied to the problem for selected flowfields.

As would be expected, the sidewall boundary-layer problem is also present in two-dimensional hydrofoil testing. Kermeen[5] and Daily[6] both used mechanical force balances to measure forces on hydrofoils. In general, their lift and pitching moment data were in good agreement with previous measurements. Although their drag measurements agreed well with the available reference data in the low angle of attack range, at larger values of α their measurements were high by as much as a factor of two. In the early 1970's, researchers, in an effort to develop new propulsor blade design criteria, used a three-component, mechanical force balance in an attempt to measure the two-dimensional sectional characteristics of a hydrofoil that spanned the rectangular test section of the ARL/PSU 12-in. (304.8-mm) cavitation tunnel.[7] With the exception of the pitching moment characteristics, the data were in disagreement with available reference data (later reorientation of the sensing elements solved the lift problem).

Although air and water are both fluids, fundamental differences exist in the testing requirements between the two media. Testing airfoil shapes in water (hydrofoils) introduces additional problems, such as the handling of larger gross forces and waterproofing requirements. However, the major concern in water tunnel measurements is the cavitation phenomenon. A hydrofoil may operate in any or all of three different flow regimes: fully wetted flow, partially cavitating flow, or fully cavitating flow. Testing in fully wetted flow differs little from low-speed wind tunnel testing, and it was this regime that was of primary concern in the original water tunnel test program.

In a water tunnel, placing pressure taps on a hydrofoil surface or on the test section walls can cause premature cavitation and result in erroneous pressure measurements. Wall boundary-layer control mechanisms are cavitation prone, and, at certain flow conditions, pressure probes in the hydrofoil wake are also subject to cavitation problems. For these reasons, water tunnel force measurements are best performed by a mechanical force balance. With such a balance, forces can be measured directly without marring the model's surface. As previously discussed, mechanical balances are not totally free of problems. Balances measure all forces applied to a model; and if forces occur on a model which are not those associated with two-dimensional flow, the balance will also measure them. A correction procedure is then required to reduce this measured total force to a two-dimensional force. However, the traditional corrections discussed by Pope[8] and Allen and Vincenti[9]—namely, solid blockage, wake blockage, lift effect, and horizontal buoyancy—are not sufficient to correct the drag data satisfactorily. Thus, a diagnostic wind tunnel test program to identify additional correction procedures was conducted. The wind tunnel provided an environment in which the aerodynamic and geometric parameters common to both airfoil and hydrofoil testing could be easily and economically varied. The results of this investigation conducted by Jacobs[10] verified that the two-dimensionality of the flow was being contaminated by the interaction of the airfoil with the sidewall boundary layer and permitted the formulation by Jacobs[10] of an empirical correction procedure which is summarized here in Eq. (12). When this correction procedure is applied to the Jacobs[10] balance-measured drag data and to additional drag data measured by Ward,[11] the results are in good agreement with the reference data.

The specific details of the entire wind tunnel test program are documented in Ref. 10. Discussed in the remainder of this paper are the portions of the test program relevant to the lift and drag measurements, the development of the correction procedure, and the application of the correction procedure to existing experimental data.

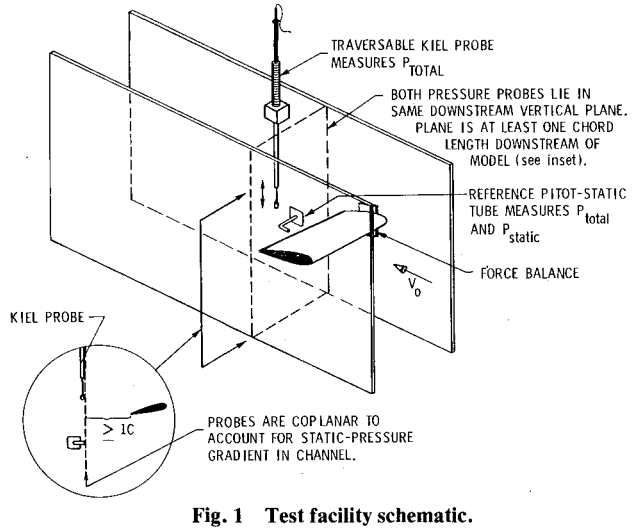

Fig. 1 Test facility schematic.

Wind Tunnel Test Program

Test Facility and Experimental Hardware

The ARL/PSU subsonic wind tunnel is a closed circuit, closed jet wind tunnel with an octagonal test section 4.0 ft (1.219 m) across the flats and is 16.0 ft (4.877 m) long. The test section velocity can be varied continuously up to 120.0 ft/s (36.576 m/s). Honeycomb and screens used in the settling section reduce the turbulence level in the test section to less than 0.10% of the freestream velocity at 80.0 ft/s (24.384 m/s). For this test program, two 4.0×8.0 ft (1.219×2.438 m) wooden panels were mounted vertically 18.375 in. (466.725 mm) apart to create a two-dimensional test section as shown in the test facility schematic, Fig. 1.

Two NACA 0012 airfoils of aspect ratios 1.02 [$c = 18.0$ in. (457.2 mm), $s = 18.375$ in. (466.7 mm)] and 2.04 [$c = 9.0$ in. (228.6 mm), $s = 18.375$ in. (466.7 mm)] were fabricated. When installed in the test chamber, the airfoil was attached at its midchord to the balance by a spanwise internal shaft. The balance shaft was located midway between the floor and ceiling of the test section and 28.0 in. (711.2 mm) downstream from the leading edge of the wooden panels.

Instrumentation

Because measurement of the pitching moment had not been a problem in the past, lift and drag forces only were measured by a two-component balance. This balance used the compact strain-gaged tension-member concept developed by Gurney.[12] The balance rotated with the airfoil and sensed forces normal to and parallel with the chordline.

For the force measurements the reference velocity V_∞ was measured by a 0.25-in. (6.35-mm) diam pitot-static probe located on the tunnel floor midway between the sidewalls and in the same vertical plane as the midchord of the airfoil. The probe tip was above the floor boundary layer.

Wake traverses to evaluate the sectional drag coefficient were conducted with a 0.125-in. (3.175-mm) diam Kiel probe located midway between the sidewalls and in a vertical plane one chord length downstream from the trailing edge of the airfoil. For these tests, the reference pitot-static probe was located in the traverse plane midway between the floor and the centerline of the test section, Fig. 1. The same Kiel probe was used to make sidewall boundary-layer measurements at the balance shaft location. For these measurements, the reference pitot-static probe in the tunnel floor was used. In all cases the reference probe was located so that it was not influenced by the deflection of the airfoil for the angles used in this study.

To obtain horizontal buoyancy corrections, the sidewall static pressure gradient was measured by four static pressure taps along the horizontal centerline of the sidewall. The angle of attack was measured with a gunners quadrant in conjunction with an accurately machined airfoil template.

Measurements and Results

Test Section Characteristics

The flow characteristics of the two-dimensional test section were established by a series of preliminary tests prior to the installation of the airfoil. Flow uniformity was verified for the region outside of the influence of the four test section boundary layers by Kiel probe surveys. The longitudinal static pressure gradient $[(dP_s/dx)/\frac{1}{2}\rho V_\infty^2]$ was measured to be 0.01236 ft^{-1} (0.0406 m^{-1}). The sidewall boundary layer at the balance shaft location was measured at several Reynolds numbers; the resulting data are presented in Fig. 2. Outside of the sidewall boundary layer, these data also demonstrate the uniformity of the flow within the test section.

Establishing a Reference Data Base

Because no reputable drag polars could be located at the target Reynolds number ($Re = 330{,}000$), new baseline data were measured as a part of the wind tunnel test program. The proven NACA approach of using separate lift and drag measurements with modern instrumentation was utilized with the 9.0-in. (228.6-mm) chord airfoil. The lift data were measured by the force balance, whereas the drag were obtained from momentum principles applied to downstream wake traverses at the midspan of the airfoil where the two-dimensionality of the flow had been verified.[10] In Fig. 3 the resulting lift data are shown in comparison with the Loftin and Smith[1] measurements at a Re of 700,000 and with computational data[13] at $Re = 330{,}000$. For completeness the balance-measured data with 18.0-in. (457.2-mm) chord airfoil are also shown. These data were judged to be in satisfactory agreement.

The resulting drag data are shown by the solid "diamonds" in Fig. 4. To establish a trend with Re, data from other sources[14,15,16] are also included in Fig. 4. The current data fit in well with the observed Re variation. It should be noted that the only reference data at the target Re are the computational data[13] and the high turbulence level data of Jacobs and Sherman.[15] The computational data predict the onset of separation but do not include the associated effects on c_ℓ and c_d in the computations and, thus, underpredict c_d at the higher c_ℓ values. For these reasons, the sectional characteristics measured by the combined balance-wake traverse approach[10] were used as the "reference data" for the remainder of the study.

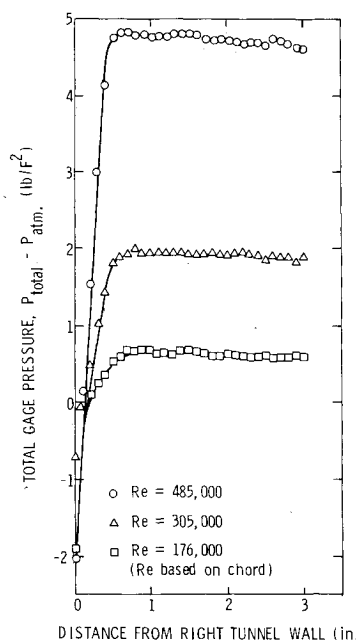

Fig. 2 Results of boundary-layer surveys at the balance shaft location.

Balance Measurements

The results of the balance measurements are shown in Figs. 3 and 5. In Fig. 5, the discrepancy, Δc_d, between the balance-measured drag and the reference data is evident.

Three possible error sources in the balance-measured drag data were considered: 1) end gap effects between the airfoil tip and the adjacent sidewall, 2) drag on the portion of the balance shaft between the sidewall and the model, and 3) contamination of the two-dimensional flow by an interaction of the airfoil and the sidewall boundary layer. The effect of the end gap between the airfoil tip and the test chamber wall

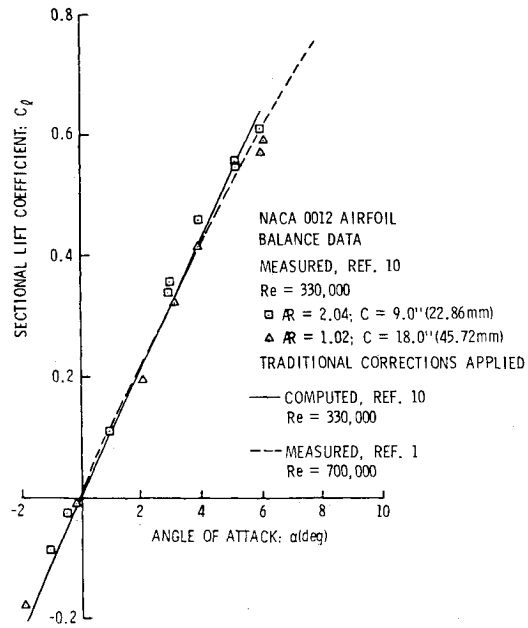

Fig. 3 Sectional lift characteristics measured by the two-component force balance.

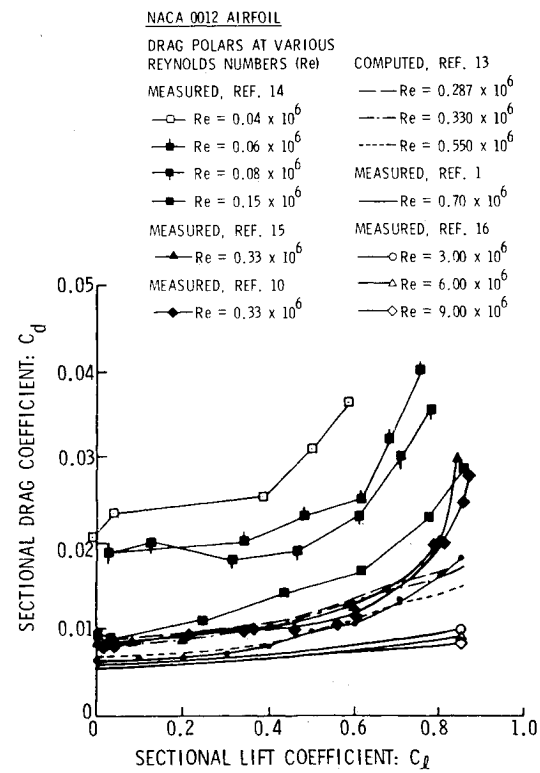

Fig. 4 Comparison of drag polars for the NACA 0012 airfoil at various Reynolds numbers.

was first investigated. Lift and drag data were measured at a constant angle of attack while varying the gap from 0.001 to 0.010 in. (0.025 to 0.254 mm). For this range of end gap, no significant change in c_d was measured and less than a 1.0% change in c_ℓ was recorded. Parkin and Kermeen[17] reported similar results, i.e., if the end gap is sufficiently small, viscous forces predominate and the effect of the end gap is negligible.

To evaluate the drag force on the portion of the balance shaft exposed to the flow a stub spindle was fabricated. The stub spindle was mounted in the balance and extended 0.002 in. (0.508 mm) into the flow. This was the typical operating clearance at the balance end of the airfoil. The 9.0-in. (228.6-mm) airfoil was mounted on the opposite wall and was maintained at a minimum distance from the spindle. Under these conditions, the flow in the vicinity of the model-sidewall intersection was closely duplicated and the balance measured only the forces on the stub spindle. The effect was negligible.

Thus, only the contamination of the two-dimensional flow by the interaction of the airfoil with the sidewall boundary layer remained as a postulated cause of the erroneous drag measurement. Evidence of such an interaction was observed during the wake measurement phase where a secondary wake was measured near the sidewall, Fig. 6. As previously discussed, the removal of the sidewall boundary layer is not practical in water tunnel applications, so the alternate approach of developing a correction procedure was chosen.

Development of the Correction Procedure

Shown in Fig. 5 is the variation between balance-measured drag data[10] and the reference two-dimensional section characteristics for the NACA 0012 airfoil. Because this difference is typical only of balance-measured data in which the entire force exerted or the airfoil/hydrofoil is measured, it was assumed that this increment in drag, Δc_d, was due to three-dimensional flow effects on the model. Such three-dimensional flow effects can be generated when a strut intersects a flat surface in the presence of a nonuniform flow. The resulting secondary flow—the so-called horseshoe vortex, Fig. 7—engulfs the strut-wall intersection and produces a region of contaminated two-dimensional flow. This type of secondary flow can be generated in airfoil/hydrofoil testing when an airfoil or hydrofoil that spans the test section intersects the test section wall in the presence of the sidewall boundary layer.

A study of this problem using flow visualization techniques was recently completed by Barber[18] in which he investigated the additional drag created by a strut protruding from a wall as a function of the incoming boundary-layer thickness. He found that the size of the horseshoe vortex varied directly with the thickness of the incoming boundary layer. He also found that the portion of the airfoil where flow separation occurred varied inversely with the size of the horseshoe vortex. He concluded that with a large horseshoe vortex, viscous effects caused high energy fluid to be entrained in the corner where the airfoil trailing edge and wall intersect, as shown in Fig. 7. This influx of high energy fluid enables the flow to withstand better the adverse pressure gradient existing in the corner and, consequently, retards flow separation. As illustrated in Fig. 7, a thin vortex is not able to entrain as much of the high energy fluid and a larger separated zone exists.

Hawthorne[19] derived the following expression for the energy in secondary flows, D_e^*, created by strut-wall inter-

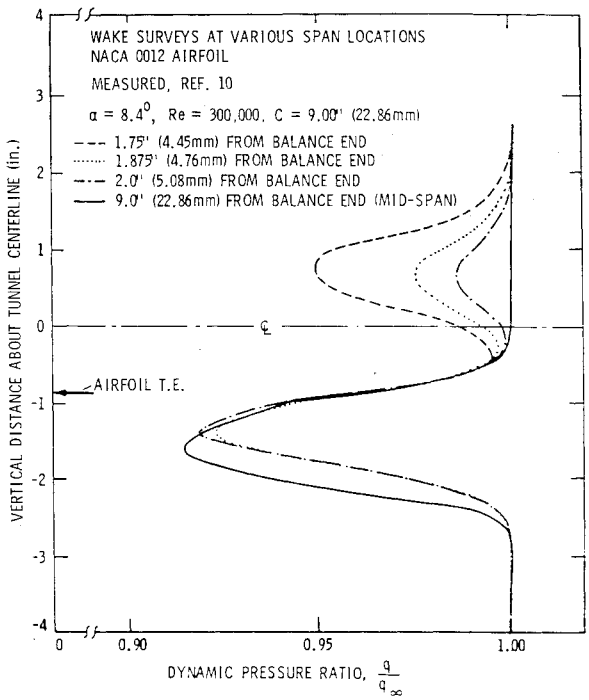

Fig. 6 Wake profiles in the vicinity of the airfoil-wall intersection showing the growth of a second wake behind the airfoils upper surface.

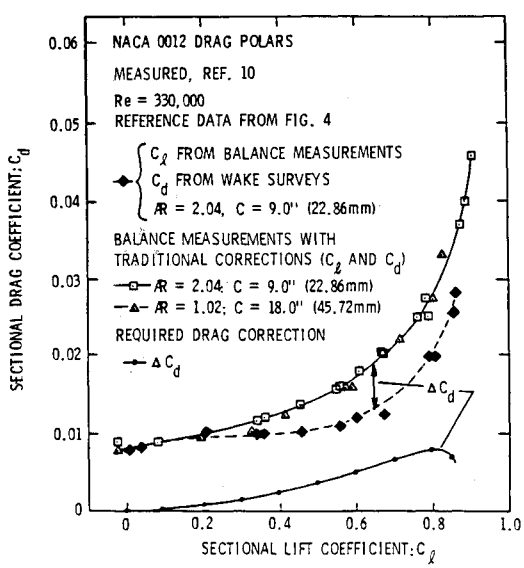

Fig. 5 Measured NACA drag polar, Ref. 10, and the required correction, Δc_d, to the drag data.

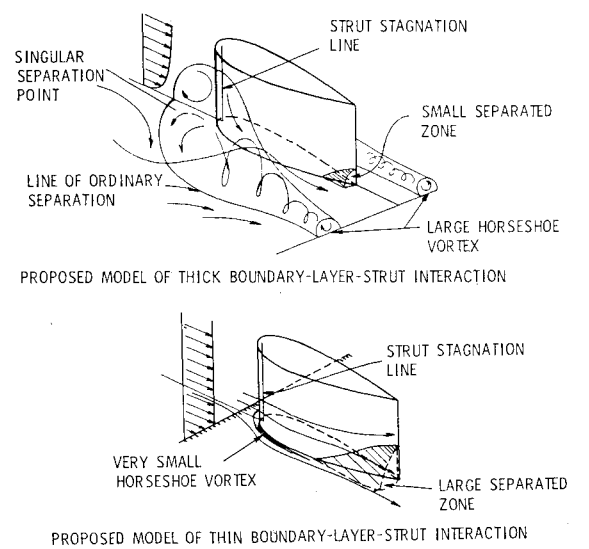

Fig. 7 Barber's model of the flow conditions occurring in the vicinity of an airfoil-tunnel wall intersection.

sections:

$$D_e^* = \frac{144 V_\infty^2 c^2 (t/c)^4 f(n)}{25[1+(1/2)/(t/c)^2]} \tag{1}$$

where

$$f(n) = \frac{n^2}{1+n^2}\frac{2}{\pi}\left\{\frac{\pi}{4n}\left(\frac{n^2-1}{n^2+1}\right)^2 + \frac{1-n^2}{(1+n^2)}\log_e n + \frac{1}{1+n^2}\right\} - \frac{1}{4n} \tag{2}$$

and

$$n = 4[1+(1/2)(t/c)]/(15\pi\delta^*/c) \tag{3}$$

Hawthorne's relationship between $f(n)$ and boundary-layer displacement thickness (δ^*/c) is shown in Fig. 8. These data are for a bicusped strut profile in an exponential boundary layer with strut thickness-to-chord ratios of 0.05 and 0.25. Hawthorne's figures show that $f(n)$ increases with δ^*/c to a maximum value at $\delta^*/c = 0.1$. Equation (1) states that the energy in these secondary flows is proportional to airfoil thickness to the fourth power and reaches a maximum when δ^*/c is approximately 0.1. Although the theory does not hold for all airfoil shapes or boundary-layer profiles, it is probably fair to assume that, in general, the energy in secondary flows for this type of airfoil/tunnel wall intersection is

$$D_e^* = K_1 (t/c)^4 f(n) \tag{4}$$

If the function $f(n)$ in Fig. 8 is linearized over the portion of the curve $0.0 \le \delta^*/c \le 0.1$, then

$$f(n) = (f(n)_{\max}/(0.1))(\delta^*/c) = K_2(\delta/c) \tag{5}$$

In Eq. (5), the displacement thickness δ^* has been assumed proportional to the more frequently documented boundary-layer thickness δ. Thus, D_e^* becomes

$$D_e^* = K_3 (t/c)^4 (\delta/c) \tag{6}$$

Funtionally, the drag correction was assumed to take the following form:

$$\Delta c_d = g_1(D_e^*, c_\ell, c_d, \alpha, \mathcal{R}) \tag{7}$$

The inverse relationship between Δc_d and D_e^* has been established by Barber.[18] Therefore, Eq. (7) can be written as

$$\Delta c_d = K_4 \frac{g_2(c_\ell, c_d, \alpha, \mathcal{R})}{(\delta/c)(t/c)^4} \tag{8}$$

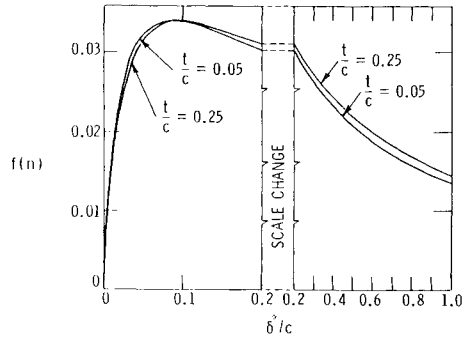

Fig. 8 Hawthorne's variation of $f(n)$ with δ^*/c [Eq. (2)] for $t/c = 0.05$ and 0.25.

The effects of c_ℓ, c_d, α, and $\mathcal{R}$ were derived empirically from the available experimental data.

The required Δc_d correction to the drag data is shown by the lower curve in Fig. 5. The deviation of drag is essentially zero at $c_\ell = 0.0$. The Δc_d curve increases to the region where c_{ℓ_α} is no longer constant and then decreases. If $c_{\ell_{\alpha-0}}$ represents the slope of the lift curve in the linear portion of the c_ℓ vs α curve, then the shape of Δc_d vs α curve seems to vary as $[c_{\ell_\alpha}/c_{\ell_{\alpha-0}}]^{1/2}$. It was assumed that this slope variation represented the angle of attack contribution to the drag correction, so that Δc_d can be expressed as

$$\Delta c_d = K_5 \frac{(c_{\ell_\alpha}/c_{\ell_{\alpha-0}})^{1/2} g_3(c_\ell, c_d, \mathcal{R})}{(\delta/c)(t/c)^4} \tag{9}$$

As the experimental data show, Δc_d increases directly with c_ℓ, and Δc_d is zero at $c_\ell = 0.0$. This also implies that the balance measures the correct value of c_d at $c_\ell = 0.0$, namely, c_{d_0}. Thus, c_{d_0} was included as the c_d term which "individualizes" the correction procedure to specific airfoils. When the linear dependence on c_ℓ and the c_{d_0} are introduced in Eq. (9), Δc_d becomes

$$\Delta c_d = K_6 \frac{c_\ell \cdot c_{d_0} (c_{\ell_\alpha}/c_{\ell_{\alpha-0}})^{1/2}}{(\delta/c)(t/c)^4} g_4(\mathcal{R}) \tag{10}$$

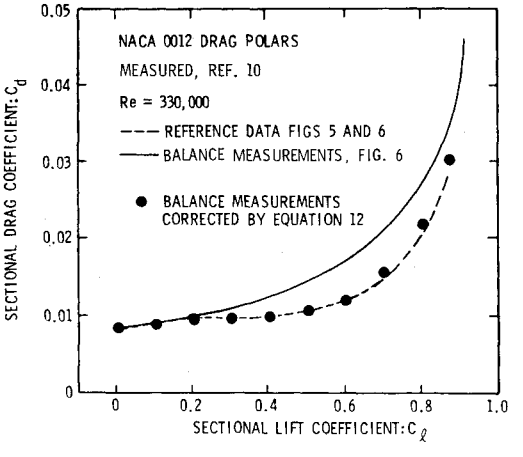

Fig. 9 NACA 0012 force balance drag polar, Ref. 10, corrected via Eq. (12).

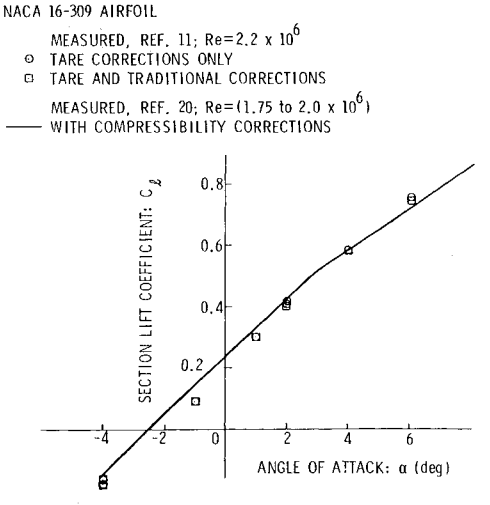

Fig. 10 Measured lift characteristics, Refs. 11 and 20, of the NACA 16-309 airfoil (hydrofoil).

The effect of aspect ratio was approximated by

$$g_4(\mathcal{R}) = (\mathcal{R})^b \tag{11}$$

The values of K_6 and b were determined empirically from the experimental data. It was found that the best fit to the data was obtained for $K_6 = 1.9\times10^{-5}$ and $b = -\frac{1}{2}$. With the evaluation of these two constants the final form of the equation to correct the balance measured drag data for the effect of the sidewall boundary layer is

$$\Delta c_d = 1.9\times10^{-5}\frac{(c_\ell)(c_{d_0})(c_{\ell_\alpha}/c_{\ell_{\alpha-0}})^{1/2}}{(\delta/c)(t/c)^4(\mathcal{R})^{1/2}} \tag{12}$$

In summary, the proposed correction to balance-measured drag data for the effect of the sidewall boundary layer is a function of the airfoil/hydrofoil geometry (t/c and $\mathcal{R}$), the thickness of the sidewall boundary layer (δ/c), and the accurately measured balance data (c_{d_0} and c_ℓ vs α).

Application and Discussion

Shown in Fig. 9 are the results of applying the correction procedure to the Jacobs[10] data. As can be seen in this figure, the corrected drag polar is in good agreement with the reference data.

In practice, this correction for the sidewall boundary layer, Eq. (12), is applied to the drag data after the tare readings and the traditional corrections have been applied. The technique will be illustrated by applying the procedure to data measured by Ward.[11] These data were located by the authors after the completion of Jacobs' initial studies and were not included in the development of Eq. (12).

Ward used a three component, mechanical balance to measure lift, drag and pitching moment on a 6.0×6.0 in. (152.4×152.4 mm) NACA 16-309 hydrofoil in the CIT High Speed Water Tunnel. The resulting noncavitating data at 50.0 ft/s (15.24 m/s) with the tare corrections included are shown by the open circles in Figs. 10 and 11. The data were further corrected according to Pope[8] for solid blockage, wake blockage, and lift effect (streamline curvature). The sidewall of the test section was adjusted to eliminate the horizontal buoyancy effect. The results of applying these traditional corrections to the data are shown by the open squares in Figs. 10 and 11. Also shown as solid lines in these figures are the NACA reference data. These data are measured by Lindsey et al.[20] with both force balance and wake survey techniques over a Re number range of 1.75×10^6 to 2.0×10^6. The data have been corrected by the methods of Ref. 8 and for compressibility effects. The required Δc_d correction for Ward's[11] data is shown by the dash-dot curve in Fig. 11. Again it is interesting to note that the balance has measured the correct drag value at the zero lift condition. From Ref. 11 the following parameters were obtained for the application of Eq. (12): $c_{d_0} = 0.0009$, $\mathcal{R} = 1.00$, $(t/c) = 0.09$. The c_ℓ term is, of course, the corrected lift coefficient (open squares) at each α. The $(c_{\ell_\alpha}/c_{\ell_{\alpha-\alpha-0}})^{1/2}$ term was computed by fitting a differentiable mathematical spline curve through the corrected c_ℓ vs α data. Ward[21] documents the test section boundary-layer characteristics of his water tunnel at the balance shaft location. The average value of δ/c at 50.0 ft/s (15.24 m/s) is 0.125. With these values Eq. (12) can now be evaluated. The resulting Δc_d values are shown as the solid squares in Fig. 11. When these computed Δc_d values are applied to Ward'd drag polar, the corrected data are shown by the solid circles. The agreement is certainly encouraging.

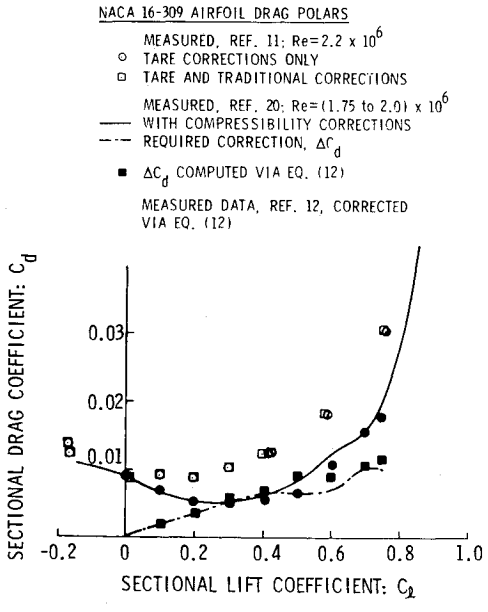

Fig. 11 NACA 16-309 force balance drag polar, Ref. 11, corrected via Eq. (12).

Conclusions

The results of the subject experimental investigation and subsequent data analysis have revealed or reaffirmed several important conclusions relative to balance-oriented two-dimensional airfoil/hydrofoil testing:

1) The effect of a small end gap between the airfoil tip and the channel wall is negligible provided the gap-to-chord ratio is ≤ 0.002.

2) For gap-to-chord ratios ≤ 0.001, the effects of flow in the region of the supporting shaft are negligible.

3) With the application of only traditional and tare corrections, valid drag polars can be obtained by combining the balance-measured c_ℓ values and c_d data from wake traverses.

4) The disagreement between the traditionally corrected balance-measured drag data and the reference values is primarily the result of the interaction of the airfoil/hydrofoil and the sidewall boundary layer.

5) The effect of the sidewall boundary layer on balance-measured drag data can be accounted for by the application of the empirically derived correction procedure.

6) The previous conclusions are not without some limitations. The empirical development of the correction procedure was conducted in the absence of data obtained from studies in which there was a significant variation in aspect ratio or thickness to chord ratio. The linearized adaptation of Hawthorne's $f(n)$ curve is only valid for $\delta^*/c \leq 0.1$. For values of $\delta^*/c > 0.1$, a different approximation of $f(n)$ would be required.

Acknowledgment

The work was supported by the Naval Sea Systems Command, Code NSEA-63R31. The authors also acknowledge the technical guidance and motivational impetus provided by Dr. B. R. Parkin, Head of the Hydromechanics Department at the Applied Research Laboratory of The Pennsylvania State University, throughout the investigation. The authors are also indebted to the Defense Research Establishment-Atlantic of Nova Scotia, Canada, for providing the NACA 16-309 hydrofoil experimental sectional characteristics.

References

[1] Loftin, L. K. and Smith, H. A., "Aerodynamic Characteristics of 15 NACA Airfoil Sections at Seven Reynolds Numbers from 0.7×10^6 to 9.0×10^6," NACA TN 1945, Oct. 1949.

[2] Barnwell, R. W., "Similarity Rule for Sidewall Boundary-Layer Effects in Two-Dimensional Wind Tunnels," *AIAA Journal*, Vol. 18, Sept. 1980, pp. 1149-1151.

[3]Sewall, W. G., "Effect of Sidewall Boundary Layers in Two-Dimensional Subsonic and Transonic Wind Tunnels," *AIAA Journal,* Vol. 20, Sept. 1982, pp. 1253-1256.

[4]Kemp, W. B., Jr. and Adcock, J. B., "Combined Four-Wall Assessment in Two-Dimensional Airfoil Tests," *AIAA Journal,* Vol. 21, Oct. 1983, pp. 1353-1359.

[5]Kermeen, R. W., "Water Tunnel Tests of NACA 4412 and Walchner Profile 7 Hydrofoils in Noncavitating and Cavitating Flows," California Institute of Technology, Rept. 47-5, Feb. 1956.

[6]Daily, J. W., "Cavitation Characteristics and Infinite Aspect Ratio Characteristics of a Hydrofoil Section," *Transaction of the ASME,* Vol. 71, April 1949, pp. 269-284.

[7]"Garfield Thomas Water Tunnel Test Facilities," Applied Research Laboratory, The Pennsylvania State University, State College Pa., Jan. 1980.

[8]Pope, A. and Harper, J. J., *Low Speed Wind Tunnel Testing,* John Wiley & Sons, New York, 1966, pp. 268-344.

[9]Allen, H. J. and Vincenti, W. G., "Wall Interference in a Two-Dimensional Flow Wind Tunnel with Consideration of the Effect of Compressibility," NACA Rept. 782, 1944.

[10]Jacobs, P. P., Jr., "A Method of Correcting for the Effects of the Sidewall Boundary Layer in Two-Dimensional Airfoil Testing," Applied Research Laboratory, The Pennsylvania State University, State College, Pa., ARL/PSU TM 80-44, March 1980.

[11]Ward, T. M., "Experiments on the NACA 16-309 Foil Section Fitted with an Adjustable Flap in Fully-Wetted and Cavitating Flows," Graduate Aeronautical Laboratories, California Institute of Technology, Rept. HSWT-1127, 1976.

[12]Gurney, G. B., "An Analysis of Force Measurement," M.S. Thesis, The Pennsylvania State University, Sept. 1962.

[13]Gregorek, G. M., computations prepared by the Airfoil Design and Analysis Center, The Ohio State University, Columbus, Ohio, Sept. 1982.

[14]Althaus, D., "Profilpolaren für den Modelflug," *Zeitlin and Verbegge,* Los Angeles, Calif., 1981, pp. 116-117.

[15]Jacobs, E. N. and Sherman, A., "Airfoil Section Characteristics as Affected by Variations of the Reynolds Number," NACA Rept. 586, 1937.

[16]Abbott, I. H., von Doenhoff, A. E. and Stivers, L. S., "Summary of Airfoil Data," NACA Rept. 824, 1945.

[17]Parkin, B. R. and Kermeen, R. W., "Water Tunnel Techniques for Force Measurements on Cavitating Hydrofoils," *Journal of Ship Research,* Vol. 1, April 1957, p. 36.

[18]Barber, T. J., "An Investigation of Strut-Wall Intersection Losses," *Journal of Aircraft,* Vol. 15, Oct. 1978, pp. 676-681.

[19]Hawthorne, W. J., "The Secondary Flow about Struts and Airfoils," *Journal of the Aeronautical Sciences,* Vol. 21, Sept. 1954, pp. 588-609.

[20]Lindsey, W. F., Stevenson, D. B., and Daley, B. N., "Aerodynamic Characteristics of 24 NACA 16 Series Airfoils at Mach Numbers between 0.3 and 0.8," NACA TN 1546, Sept. 1948.

[21]Ward, T. M., "The Hydrodynamics Laboratory at The California Institute of Technology—1976," *Journal of Fluids Engineering,* Dec. 1976, p. 742.